Propagation of elastic waves in a fluid-loaded anisotropic functionally graded waveguide: Application to ultrasound characterization of cortical bone

Cécile Baron and Salah Naili

Laboratoire de Mécanique Physique, UMR CNRS 7052, B2OA
Faculté des Sciences et Technologie, Université Paris 12 – Val de Marne
61, Avenue du Général de Gaulle, 94010 Créteil cedex, FRANCE

E-mail: cecile.baron@univ-paris12.fr, naili@univ-paris12.fr

Abstract Non-destructive evaluation of heterogeneous materials is of major interest not only in industrial but also in biomedical fields. In this work, the studied structure is a three-layered one: a laterally heterogeneous anisotropic solid layer is sandwiched between two acoustic fluids. An original method is proposed to solve the wave equation in such a structure without using a multilayered model for the plate. This method is based on an analytical solution, the matricant, explicitly expressed under the Peano expansion form. We validate this approach for the study of a fluid-loaded anisotropic plane waveguide with two different fluids on each side. This configuration corresponds to the axial transmission technique to the ultrasound characterization of cortical bone *in vivo*.

1 Introduction

A lot of natural media have unidirectional varying elastic properties. The mantel crust, the oceans and cortical bone are some of these functionally graded media. Scientists focused on the advantages presented by this type of materials in terms of mechanical behavior and since the 80's, they developed industrial Functionally Graded Materials (FGM) particularly exploited in high-technology and biomedical applications. Consequently, the non-destructive evaluation of these materials is a key issue. Surface and guided waves play a major role in non-destructive testing and evaluation of complex structures. Several studies are dedicated to the leaky Lamb wave propagation in fluid-loaded plates [1, 2, 3]. In all these studies, the media are homogeneous or multilayered. In this work, we introduce a general method to take into account the continuous property variation in an anisotropic waveguide. This method is based on the knowledge of an analytical solution of the wave equation, the matricant, explicitly expressed *via* the Peano series. To the best of our knowledge, this is the first method to evaluate the mechanical behavior of a fluid-loaded anisotropic waveguide with continuously varying properties without modelling the FGM plate as a multilayered plate.

In this work, we first present the method and its setup with fluid-structure interaction; then we proceed to the validation of the method by comparing our results to the dispersion curves obtained from classical schemes on homogeneous waveguides (isotropic and anisotropic). Two advantages of the method are underlined: i) an asymmetric fluid-loading may be taken into account without modifying the scheme for the numerical solution; ii) the influence of the property gradient on the mechanical behavior of the waveguide may be investigated. Finally, we get onto the relevancy of this model applied to the ultrasound characterization of cortical bone by the axial transmission technique.

2 General formulation of the problem

We consider an elastic parallel plate waveguide of thickness d sandwiched between two perfect fluids f_1 and f_2, of respective mass densities ρ_{f_1} and ρ_{f_2}, and, of respective velocities c_{f_1} and c_{f_2}. The interfaces between the fluids and the plate are infinite planes parallel to the $(\mathbf{x}_1, \mathbf{x}_2)$-plane. Therefore, we assume that the structure is two-dimensional and that the guided waves travel in the plane $x_2 = 0$ (see Fig. 1); in the following parts, this coordinate is implicit and is omitted in the mathematical expressions.

The elastic plate is supposed to be anisotropic and is liable to present continuously varying properties along its thickness ($\mathbf{x}_3$-axis). These mechanical properties are represented by the elasticity tensor $\mathbb{C} = \mathbb{C}(x_3)$ and the mass density $\rho = \rho(x_3)$.

2.1 System equations

2.1.1 The wave equation in the fluid f_n (for $n = 1$ or 2)

In the fluid f_n, the characteristic equations are written as:

$$\begin{cases} \dfrac{\partial p^{(n)}}{\partial x_j} = \rho_{f_n} \dfrac{\partial^2 u_j^{(n)}}{\partial t^2}, \\ p^{(n)} = K_{f_n} \texttt{div}\ \mathbf{u}^{(\mathbf{n})}, \end{cases} \tag{1}$$

where $\mathbf{u}^{(n)}$ and $p^{(n)}$ respectively represent the displacement vector and the pressure in the fluid f_n; its compressibility and velocity are respectively K_{f_n} and $c_{f_n} = \sqrt{K_{f_n}/\rho_{f_n}}$. The operator `div` is the divergence.

The solutions of the system (1) for the fluid f_n are sought under the form:

$$\mathbf{f}_n(x_1, x_2; t) = \mathbf{A}_n(x_3) \exp \imath(k_1 x_1 + k_3^{(n)} x_3 - \omega t), \tag{2}$$

where k_1 is the wavenumber along the $\mathbf{x}_1$-axis, $k_3^{(n)}$ is the wavenumber along the $\mathbf{x}_3$-axis in the fluid f_n and ω is the angular frequency.

We consider an incident wave reaching the plate at an angle θ_1 from the $\mathbf{x}_3$-axis in the fluid f_1. The incident displacement-field is defined in the following form, assuming that its amplitude is normalized:

$$\mathbf{u}_I^{(1)} = \begin{pmatrix} \sin\theta_1 \\ 0 \\ \cos\theta_1 \end{pmatrix} \exp \imath(k_1 x_1 + k_3^{(1)} x_3 - \omega t), \tag{3}$$

with $\sin\theta_1 = k_1 c_{f_1}/\omega$ and $\cos\theta_1 = k_3^{(1)} c_{f_1}/\omega$. From this, the expression of the reflected displacement-field $\mathbf{u}_R^{(1)}$ in f_1 and of the transmitted displacement-field $\mathbf{u}_T^{(2)}$ in f_2 are deduced:

$$\mathbf{u}_R^{(1)} = R \begin{pmatrix} \sin\theta_1 \\ 0 \\ -\cos\theta_1 \end{pmatrix} \exp \imath(k_1 x_1 - k_3^{(1)} x_3 - \omega t), \quad \mathbf{u}_T^{(2)} = T \frac{c_{f_2}}{c_{f_1}} \begin{pmatrix} \sin\theta_1 \\ 0 \\ \cos\theta_1 \end{pmatrix} \exp \imath(k_1 x_1 + k_3^{(2)} x_3 - \omega t). \tag{4}$$

The incident, reflected and transmitted pressure fields, respectively noted $p_I^{(1)}$, $p_R^{(1)}$ and $p_T^{(2)}$ are deduced from the expressions (3) and (4) and the second equation of the system (1).

2.1.2 The wave equation in the plate waveguide

The body forces in the solid plate are neglected. The momentum conservation equation associated with the constitutive law of linear elasticity (Hooke's law) gives the following equations:

$$\begin{cases} \dfrac{\partial \sigma_{ij}}{\partial x_j} = \rho \dfrac{\partial^2 u_i}{\partial t^2}, \\ \sigma_{ij} = \dfrac{1}{2} C_{ijk\ell} \left(\dfrac{\partial u_k}{\partial x_\ell} + \dfrac{\partial u_\ell}{\partial x_k} \right) \end{cases} \tag{5}$$

where u_i (for $i = 1, ..., 3$) and σ_{ij} (for $i, j = 1, ..., 3$) respectively represent the components of the displacement-field $\mathbf{u}$ and of the stress $\boldsymbol{\sigma}$. The solutions are sought for the vectors of displacement $\mathbf{u}$ and traction σ_{i3} (for $i = 1, ..., 3$) (assumed to be harmonic in time t and space along the $\mathbf{x}_1$-axis) under the form:

$$\mathbf{f}(x_1, x_3; t) = \mathbf{A}(x_3) \exp \imath (k_1 x_1 - \omega t), \tag{6}$$

2.1.3 Fluid-loading interface conditions

The conditions at both interfaces $x_3 = 0$ and $x_3 = d$ are the continuity of the normal displacement and the one of the normal stresses. We consider that the fluids f_1 and f_2 are perfect, consequently, the shear stresses are zero at the interfaces ($\sigma_{13}(x_1, 0; t) = \sigma_{13}(x_1, d; t) = 0$ and $\sigma_{23}(x_1, 0; t) = \sigma_{23}(x_1, d; t) = 0$). The following relations are obtained:

$$\begin{cases} u_3(x_1, 0; t) = u_3^{(1)}(x_1, 0; t), \quad u_3(x_1, d;\ t) = u_3^{(2)}(x_1, d; t), \\ \sigma_{33}(x_1, 0; t) = p^{(1)}(x_1, 0; t), \quad \sigma_{33}(x_1, d; t) = p^{(2)}(x_1, d; t). \end{cases} \tag{7}$$

2.2 A closed-form solution: the matricant

Introducing the expression (6) in the equation (5), we obtain the wave equation under the form of a second-order differential equation with non-constant coefficients. For particular forms of geometrical profiles, this equation has analytical solutions expressed with special functions (Bessel or Hankel functions) [4]. But in the general case, there is no analytical solution to the problem thus formulated. The most current methods to solve the wave equation in unidirectionally heterogeneous media are derived from the Thomson-Haskell method [5, 6]. These methods are appropriate for multilayered media [7, 8, 9, 10]. But, for continuously varying media, these techniques mean to replace the continuous profiles of properties by step-wise functions. Thereby the studied problem becomes an approximate one, even before the resolution step; the accuracy of the solution as its validity domain are hard to evaluate. Moreover, the multilayered model of the waveguide creates some "virtual" interfaces likely to induce artefacts. In order to deal with the exact problem, that is to keep the continuity of the properties variation, the wave equation is re-written under the form of an ordinary differential equations system with non-constant coefficients for which an analytical solution exists: the matricant [11].

We consider that the plate presents material symmetries which allow to decouple the P-SV (Pressure - Shear Vertical) waves, polarized in the propagation plane $(\mathbf{x}_1, \mathbf{x}_3)$ and the SH (Shear Horizontal) waves polarized along $\mathbf{x}_2$-axis. The incident media f_1 is a perfect fluid, only the P-SV waves travel in the plate. Applying a spatio-temporal Fourier transform on (x_1, t) of the displacement field (noted $\hat{\mathbf{u}}(k_1, x_3; \omega)$) and on the traction field (noted $\hat{\sigma}_{i3}(k_1, x_3; \omega)$ for $i = 1, ..., 3$), the wave equation becomes a matrix system expressed using the Thomson-Haskell parametrization of the Stroh formalism [12] and the Voigt notation ($C_{ijk\ell}$ for $i, j, k, \ell = 1, ..., 3$ is replaced by c_{IJ} for $I, J = 1, ..., 6$):

$$\frac{d}{dx_3}\boldsymbol{\eta}(x_3) = \imath\omega\mathbf{Q}(x_3)\boldsymbol{\eta}(x_3), \tag{8}$$

that is

$$\frac{d}{dx_3}\begin{pmatrix} \imath\omega\hat{u}_1 \\ \imath\omega\hat{u}_3 \\ \hat{\sigma}_{13} \\ \hat{\sigma}_{33} \end{pmatrix} = \imath\omega \begin{pmatrix} 0 & s_1 & 1/c_{55}(x_3) & 0 \\ -c_{13}(x_3)/c_{33}(x_3)s_1 & 0 & 0 & 1/c_{33}(x_3) \\ \rho(x_3) - s_1^2\zeta(x_3) & 0 & 0 & -c_{13}(x_3)/c_{33}(x_3)s_1 \\ 0 & \rho(x_3) & -s_1 & 0 \end{pmatrix} \begin{pmatrix} \imath\omega\hat{u}_1 \\ \imath\omega\hat{u}_3 \\ \hat{\sigma}_{13} \\ \hat{\sigma}_{33} \end{pmatrix}, \tag{9}$$

with the relations:

$$\zeta(x_3) = c_{11}(x_3) - \frac{c_{13}^2(x_3)}{c_{33}(x_3)}, \quad k_1 = \omega s_1, \tag{10}$$

where s_1 is the x_1-component of the slowness. The matrix $\mathbf{Q}$ includes all the information about the heterogeneity of the waveguide because it is expressed from the plate mechanical properties $(\rho(x_3), \mathbb{C}(x_3))$ and from two acoustical parameters (s_1, ω). The wave equation thus formulated has an analytical solution expressed between a reference point $(x_1, 0, x_3^0)$ and some point of the plate $(x_1, 0, x_3)$ in the propagation plane. This solution is called the matricant and is explicitly written under the form of the Peano series expansion:

$$\mathbf{M}(x_3, x_3^0) = \mathbf{I} + (\imath\omega)\int_{x_3^0}^{x_3} \mathbf{Q}(\xi)d\xi + (\imath\omega)^2 \int_{x_3^0}^{x_3} \mathbf{Q}(\xi)\Big(\int_{x_3^0}^{\xi} \mathbf{Q}(\xi_1)d\xi_1\Big)d\xi + ..., \tag{11}$$

where $\mathbf{I}$ is the identity matrix of dimension $(4, 4)$. We underline that the $\imath\omega$-factorization leads up to a polynomial form of the matricant. The $\imath\omega$-polynomial coefficients are matrices independent of ω.

Using the propagator property of the matricant through the plate thickness, the state-vector (defined in (9)) at the second interface $\boldsymbol{\eta}(d)$ is evaluated from the state-vector at the first interface $\boldsymbol{\eta}(0)$ as follows:

$$\boldsymbol{\eta}(d) = \mathbf{M}(d, 0)\boldsymbol{\eta}(0). \tag{12}$$

The fluid-structure interaction is taken into account *via* the interface conditions (7) used after a spatio-temporal Fourier transform on (x_1, t). The condition to obtain a non-trivial solution to the equation (12) leads to the following relation:

$$\imath\omega\hat{u}_1(k_1, 0; \omega) \times M_{13} + \imath\omega\hat{u}_3(k_1, 0; \omega) \times M_{32} + \hat{\sigma}_{33}(k_1, 0; \omega) \times M_{34} = 0, \tag{13}$$

where M_{ij} (for $i, j = 1, ..., 4$) represent the components of the matrix $\mathbf{M}$. The displacement component $\hat{u}_1(k_1, 0; \omega)$ can be expressed as a linear combination of $\hat{u}_3(k_1, 0; \omega)$ and $\hat{\sigma}_{33}(k_1, 0; \omega)$ and thus the system (12) of dimension 4 is reduced to a matrix system of dimension 2:

$$\boldsymbol{\eta}(d) = \begin{pmatrix} P_1 & P_2 \\ P_3 & P_4 \end{pmatrix} \boldsymbol{\eta}(0), \qquad \text{where } \boldsymbol{\eta}(x_3) = \begin{pmatrix} \imath\omega\hat{u}_3 \\ \hat{\sigma}_{33} \end{pmatrix}. \tag{14}$$

with the relations:

$$P_1 = M_{22} - M_{21}\frac{M_{32}}{M_{31}}, \quad P_2 = M_{24} - M_{21}\frac{M_{34}}{M_{31}}, \quad P_3 = M_{42} - M_{41}\frac{M_{32}}{M_{31}}, \quad P_4 = M_{44} - M_{11}\frac{M_{34}}{M_{31}}. \quad (15)$$

The interface conditions (7) are transformed in the Fourier domain (k_1, ω). The expressions of the displacement and the pressure in the fluids, so that the one of the displacement and traction fields in the solid plate (14), are substituted in the transformed interface conditions. We obtain the following matrix equation:

$$\begin{pmatrix} \imath\omega s_3^{(1)} c_{f_1} & 1 & 0 & 0 \\ \imath\omega\rho_{f_1} c_{f_1} & 0 & 1 & 0 \\ 0 & P_1 & P_2 & -\imath\omega s_3^{(2)} c_{f_2} \exp\left(\imath\omega s_3^{(2)} d\right) \\ 0 & P_3 & P_4 & -\imath\omega\rho_{f_2} c_{f_2} \exp\left(\imath\omega s_3^{(2)} d\right) \end{pmatrix} \begin{pmatrix} R \\ \alpha_1 \\ \alpha_2 \\ T \end{pmatrix} = \begin{pmatrix} \imath\omega s_3^{(1)} c_{f_1} \\ \imath\omega\rho_{f_1} c_{f_1} \\ 0 \\ 0 \end{pmatrix}, \quad (16)$$

where $\mathbf{s}^{(n)} = \mathbf{k}^{(n)}/\omega$ is the slowness-vector in the fluid f_n ($n = 1$ or 2); the quantities α_1 and α_2 are respectively the amplitudes of the displacement-field and of the traction-field in the waveguide at the interface $x_3 = 0$. We deduce the analytical expressions of the complex reflection and transmission coefficients ($\hat{R}(s_1, x_3; t)$ and $\hat{T}(s_1, x_3; t)$ respectively):

$$\hat{R} = \frac{(P_3 - P_1 Z_2 + P_4 Z_1 - P_2 Z_1 Z_2)}{(P_3 - P_1 Z_2 - P_4 Z_1 + P_2 Z_1 Z_2)}, \quad \hat{T} = \frac{-2Z_2(\rho_{f_1} c_{f_1}/\rho_{f_2} c_{f_2})(P_1 P_4 - P_2 P_3)}{(P_3 - P_1 Z_2 - P_4 Z_1 + P_2 Z_1 Z_2)} \exp(-\imath\omega s_3^{(2)} d), \quad (17)$$

with $Z_n = \rho_{f_n}/\sqrt{1/c_{f_n}^2 - s_1^2}$ (for $n = 1$ or 2).

3 Validation

The aim of this sub-section is to check that the Peano expansion of the matricant is well-adapted to study fluid-loaded waveguides. We take into account the fluid-structure interaction in different configurations of homogeneous plates comparing the results obtained from the numerical implementation of the Peano expansion of the matricant to results taken from the literature.

The numerical evaluation of P_1, P_2, P_3 and P_4 requires us to truncate the Peano series and to numerically calculate the integrals (by the Simpson's method of order 2). Thus, the error can be estimated and controlled [11]. The expressions (17) give the frequency spectrum (modulus and phase) of the reflection coefficient for different incidences (s_1 varies from zero – normal incidence – to $1/c_{f_1}$ corresponding to the critical incidence in the fluid f_1). A lot of works detailed the relationship between the poles and the zeros of the reflection coefficient and the leaky Lamb waves dispersion curves [1, 3].

The results of sub-section 3.1 compare the dispersion curves obtained by seeking the poles of the reflection coefficient (17) and the results taken from the literature or from closed-form solution.

3.1 Validation for a homogeneous and isotropic or anisotropic fluid-loaded plate

The method is tested by plotting the dispersion curves (variation of the phase velocity *versus* frequency-thickness product) for an isotropic aluminium plate immersed in water. The data in the paper of Chimenti and Rokhlin [1] is used. The results obtained (not shown) by the present method are in perfect agreement with the results presented by them [1].

Taking into account the anisotropy does not change the scheme for the numerical solution of wave equation with the matricant. We consider a transverse isotropic plate immersed in water. For that configuration, Nayfeh and Chimenti [13] developed a method to obtain an analytical solution. By using the data from this paper, the results obtained (not shown) with the present method are in perfect agreement with theirs.

3.2 Asymmetric loading and heterogeneous waveguide

The formalism presented here to solve the wave equation in an unidirectionally graded medium presents two main advantages: without changing the scheme to obtain the numerical solution we can take into account i) an asymmetric loading and ii) the unidirectional continuous heterogeneity.

3.2.1 Isotropic homogeneous plate and asymmetric loading ($f_1 \neq f_2$)

The mechanical behavior of the plate is different for symmetric and asymmetric loadings. For example, in the symmetric loading case, there is a unique critical frequency and a unique phase velocity value $\mathtt{v}_\varphi$ in the plate, which corresponds to the propagation velocity in the fluid ($\mathtt{v}_\varphi = c_{f_1} = c_{f_2}$), for which the displacements and the stresses at the interfaces are quasi-null; whereas in the asymmetric loading ($f_1 \neq f_2$), there are two critical frequencies and two values of the phase velocity in the plate for which the structure does not respond [14]. The validation is done on an isotropic aluminium plate with the following properties: $\rho = 2.79$ g.cm^{-3} ; the longitudinal and transverse waves velocities are respectively $\mathtt{v}_L = 6.38$ mm.μs^{-1} and $\mathtt{v}_T = 3.10$ mm.μs^{-1}. The characteristic properties of the fluid f_1 correspond to those of water: $\rho_{f_1} = 1$ g.cm^{-3} and $c_{f_1} = 1.485$ mm.μs^{-1}; the characteristic properties of the fluid f_2 correspond to glycerine: $\rho_{f_2} = 1.26$ g.cm^{-3} and $c_{f_2} = 1.920$ mm.μs^{-1}. This configuration is the same as the one studied by Franklin et al. [15]. The modulus of the reflection coefficient *versus* the incident angle is plotted in the Fig. 2 for a fixed frequency-thickness product ($f \times d = 4.7$ MHz.mm).

This figure shows the perfect agreement between our results and the ones presented by Franklin et al. [15].

3.2.2 Influence of the property gradient on the frequency spectrum of the reflection coefficient

The main characteristic of the formalism developed in this study is the possibility to take into account a continuous variation of the mechanical properties of a structure along one space direction (here, it is the thickness of the waveguide). The influence of a linear gradient of properties (corresponding to a 10%-increase of the porosity and a 10%-decrease of the propagation velocities) in a transverse isotropic bone plate immersed in water is investigated. Its properties are reported in Tab. 1. The frequency spectrum of the reflection coefficient is plotted in Fig. 3 for an incidence close to the critical incidence of longitudinal waves in the plate, which corresponds to the formation of the wave called lateral wave [16] ($\theta_1 \sim 21.93$ degrees (thin grey line and grey crosses) and $\theta_1 \sim 23.08$ degrees (thin black line)).

	ρ (g.cm^{-3})	C_{11} (GPa)	$C_{22} = C_{33}$ (GPa)	$C_{13} = C_{12}$ (GPa)	C_{44} (GPa)	$C_{55} = C_{66}$ (GPa)
$x_3 = 0$	1.9	30.04	24.6	10	6.16	9.2
$x_3 = d$	1.81	23.18	18.98	7.72	4.75	7.1

Table 1: Elastic properties of transverse isotropic bone plate with linearly varying properties along the $\mathbf{x}_3$-axis between the planes $x_3 = 0$ and $x_3 = d$.

This figure shows evidence that the behavior of the reflection coefficient modulus is sensibly the same for frequencies between 0 and 1.8 MHz. Beyond this value, the behavior is clearly different.

4 Perspectives

From this study, the transient response of a fluid-loaded plate is considered. The frequency spectrum of the reflection coefficient is calculated for incidences between the normal and critical incidences for compression waves in the fluid f_1. Thus, the plate transfer function is calculated in the Fourier domain (x_1-wavenumber, frequency): $\hat{R}(k_1, x_3; \omega)$. A double inverse Fourier transform on (k_1, ω) is applied on $\hat{R}(k_1, x_3; \omega)$ to transform into the space-time domain; the temporal signals can be obtained at different points along the propagation $\mathbf{x}_3$-axis: $R(x_1, x_3; t)$.

Lastly, the formalism presented here is well-adapted to deal with wave propagation in anisotropic tubes with radial property gradients [17]. The wave equation keeps the same form as (8), the state vector is expressed from the displacement and traction components in the cylindrical basis and the matrix $\mathbf{Q}$ depends on the radial position r ($\mathbf{Q} = \mathbf{Q}(r)$). In cylindrical homogeneous structures, to take into account an anisotropy more important than transverse isotropy is fussy because there is no analytical solution to the "classical" wave equation (second-order differential equation). The Stroh's formalism (hamiltonian formulation of the wave equation) [12], upon which the Peano expansion of the matricant is based, is a promising alternative solution which allows to consider altogether the geometry (cylinder), the anisotropy and the heterogeneity (radial property gradients) of a medium.

4.1 Relevancy of the method for ultrasound characterization of cortical bone by axial transmission technique

Several studies of demonstrated the heterogeneous nature of the cortical bone, particularly they show evidence the gradual variation of the volumetric porosity (ratio between pores and total volume) across the cortical thickness. Yet, the porosity is intrinsically linked to the macroscopic mechanical behavior of the cortical bone [18]. Therefore, the continuous variation of porosity induces a continuous variation of material properties. Taking into account the gradient should prove itself to be essential in the context of diagnosis and therapeutic monitoring of osteoporosis. Indeed, the gradient characterization would allow to assess geometrical (cortex thickness) and material (elastic coefficients variation) information, which are fundamental parameters to evaluate the bone fragility. For several years, the quantitative ultrasonography (by axial and transverse transmissions) proved itself to be an alternative hopeful technique to evaluate the fracture risk [19]. However, the inter-individual and inter-site variations of bone mechanical properties make the standardization of the protocol of fracture risk evaluation by ultrasound very delicate. In this context, the characterization of a relative variation of mechanical properties in the plate thickness may turn out to be relevant to carry out a "standardized" estimation of bone strength. The axial transmission technique is specially dedicated to the ultrasound characterization of the cortical bone, which represents 80% of the bone mass in human skeleton, in bone pathologies diagnosis. The corresponding configuration may be modelled by a cortical bone plate with varying properties in the thickness and sandwiched between two different fluids, soft tissues and marrow. According to the results presented in this study, the signals recorded by axial transmission technique, corresponding to the waves reflected by the plate and travelling into the fluid (soft tissues), are sensitive to the gradient (see Fig. 3) and may be exploited to its characterization, then to evaluate the bone fragility. To do so, a parametric study must be carried out to determine which ultrasound parameters, accessible by the axial transmission technique, are the most representative of the property gradients (which modes, at which frequencies ?). When the gradient will be characterized, the second step will be to elaborate a standardized and reliable protocol to evaluate the bone strength by ultrasound measurements in preparation for a clinical application.

References

[1] D. E. Chimenti and S.I. Rokhlin. Relationship between leaky Lamb modes and reflection coefficient zeroes for a fluid-coupled elastic layer. *Journal of Acoustical Society of America*, 88:1603–1611, 1990.

[2] D. E. Chimenti and A. H. Nayfeh. Ultrasonic Reflection and Guided Waves in Fluid-Coupled Composite Laminates. *Journal of Nondestructive Evluation*, 9:51–69, 1990.

[3] M. Deschamps and O. Poncelet. Transient Lamb waves: Comparison between theory and experiment. *Journal of Acoustical Society of America*, 107:3120–3129, 2000.

[4] V. Vlasie-Belloncle and M. Rousseau. Effect of a velocity gradient on the guided modes of a structure. In *Proceedings of the 5th World Congress on Ultrasonics*, Paris, 7-10 Septembre 2003.

[5] W. T. Thomson. Transmission of elastic waves through a stratified solid medium. *Journal of Applied Physics*, 21:89–93, 1950.

[6] N. A. Haskell. The dispersion of surface waves on multilayered media. *Bulletin of the Seismological Society of America*, 43:377–393, 1953.

[7] E. G. Kenneth. A propagator matrix method for periodically stratified media. *Journal of Acoustical Society of America*, 73(1):137–142, 1982.

[8] D. Lévesque and L. Piché. A robust transfer matrix simulation for ultrasonic response of multilayered absorbing media. *Journal of Acoustical Society of America*, 92(1):452–467, 1992.

[9] L. Wang and S. I. Rokhlin. Stable reformulation of transfer matrix method for wave propagation in layered anisotropic media. *Ultrasonics*, 39:413–424, 2001.

[10] B. Hosten and M. Castaings. Surface impedance matrices to model the propagation in multilayered media. *Ultrasonics*, 41:501–507, 2003.

[11] C. Baron. *Le développement en série de Peano du matricant pour l'étude de la propagation d'ondes en milieux continûment variables*. PhD thesis, Université Bordeaux 1, France, 2005.

[12] A. N. Stroh. Steady state problems in anisotropic elasticity. *Journal of Mathematics and Physics*, 41: 77–103, 1962.

[13] A. H. Nayfeh and D. E. Chimenti. Free Wave Propagation in Plates of General Anisotropic Media. *Journal of Applied Mechanics*, 56:881–886, 1989.

[14] J. Dickey, G Maidanik, and H. Uberall. The splitting of dispersion curves for the fluid-loaded plate. *Journal of Acoustical Society of America*, 98:2365–2367, 1995.

[15] H. Franklin, E. Danila, and J.-M. Conoir. S-matrix theory applied to acoustic scattering by asymmetrically fluid-loaded elastic isotropic plates. *Journal of Acoustical Society of America*, 110:243–253, 2001.

[16] E. Camus, M. Talmant, G. Berger, and P. Laugier. Analysis of the axial transmission technique for the assessment of skeletal status. *Journal of the Acoustical Society of America*, 108(6):3058–3065, 2000.

[17] A.L. Shuvalov. A sextic formalism for three-dimensional elastodynamics of cylindrically anisotropic radially inhomogeneous materials. *Proceedings of the Royal Society of London A.*, 459:1611–1639, 2003.

[18] C. Baron, M. Talmant, and P. Laugier. Effect of porosity on effective diagonal stiffness coefficients (c_{ii}) and anisotropy of cortical at 1 MHz: A finite-difference time domain study. *Journal of Acoustical Society of America*, 122:1810–1817, 2007.

[19] F. Marin, J. Gonzales-Macias, A. Diez-Perez, S. Palma, and M. Delgado-Rodriguez. Relationship Between Bone Quantitative Ultrasound and Fractures: a Meta-Analysis. *Journal of Bone and Mineral Research*, 21:1126–1135, 2006.

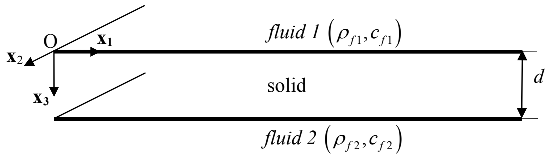

Figure 1: Geometrical configuration of the waveguide.